JOURNAL OF AIRCRAFT
Vol. 41, No. 1, January–February 2004

Lifting-Line Analysis for Twisted Wings and Washout-Optimized Wings

W. F. Phillips*
Utah State University, Logan, Utah 84322-4130

A more practical form of the analytical solution for the effects of geometric and aerodynamic twist (washout) on the low-Mach-number performance of a finite wing of arbitrary planform is presented. This infinite series solution is based on Prandtl's classical lifting-line theory and the Fourier coefficients are presented in a form that only depends on wing geometry. The solution shows that geometric and aerodynamic washout do not affect the lift slope for a wing of any planform shape. This solution also shows that any wing with washout always produces induced drag at zero lift. Except for the special case of an elliptic planform, washout can be used to reduce the induced drag for a wing producing finite lift. A relation describing the optimum spanwise distribution of washout for a wing of arbitrary planform is presented. If this optimum washout distribution is used, a wing of any planform shape can be designed for a given lift coefficient to produce induced drag at the same minimum level as an elliptic wing with the same aspect ratio and no washout.

Nomenclature

A_n	=	coefficients in the infinite series solution to the lifting-line equation
a_n	=	planform contribution to the coefficients in the infinite series solution to the lifting-line equation
b	=	wingspan
b_n	=	washout contribution to the coefficients in the infinite series solution to the lifting-line equation
C_{Di}	=	induced-drag coefficient
C_L	=	lift coefficient
C_{Ld}	=	design lift coefficient
$C_{L,\alpha}$	=	wing lift slope
$\tilde{C}_{L,\alpha}$	=	airfoil section lift slope
c	=	wing section chord length
R_A	=	wing aspect ratio
R_T	=	wing taper ratio
V_∞	=	magnitude of the freestream velocity
z	=	spanwise coordinate
α	=	geometric angle of attack relative to the freestream
α_{L0}	=	airfoil section zero-lift angle of attack
Γ	=	spanwise section circulation distribution
γ_t	=	strength of shed vortex sheet per unit span
ε_Ω	=	washout effectiveness
θ	=	change of variables for the spanwise coordinate
κ_D	=	planform contribution to the induced-drag factor
κ_{DL}	=	lift-washout contribution to the induced-drag factor
κ_{Do}	=	optimum induced-drag factor
$\kappa_{D\Omega}$	=	washout contribution to the induced-drag factor
κ_L	=	lift slope factor
Ω	=	maximum total washout, geometric plus aerodynamic
Ω_{opt}	=	optimum total washout to minimize induced drag
ω	=	normalized washout distribution function

Introduction

PRANDTL'S classical lifting-line theory[1,2] can be used to obtain an infinite series solution for the spanwise distribution of vorticity generated on a finite wing. If the circulation about any section of the wing is $\Gamma(z)$ and the strength of the shed vortex sheet per unit span is $\gamma_t(z)$, as shown in Fig. 1, then Helmholtz's vortex theorem requires that the shed vorticity is related to the bound vorticity according to

$$\gamma_t(z) = -\frac{\mathrm{d}\Gamma}{\mathrm{d}z} \tag{1}$$

For a finite wing with no sweep or dihedral, combining this relation with the circulation theory of lift produces the fundamental equation that forms the foundation of Prandtl's lifting-line theory:

$$\frac{2\Gamma(z)}{V_\infty c(z)} + \frac{\tilde{C}_{L,\alpha}}{4\pi V_\infty}\int_{\zeta=-b/2}^{b/2} \frac{1}{z-\zeta}\left(\frac{\mathrm{d}\Gamma}{\mathrm{d}z}\right)_{z=\zeta}\mathrm{d}\zeta = \tilde{C}_{L,\alpha}[\alpha(z) - \alpha_{L0}(z)] \tag{2}$$

In Eq. (2) α and α_{L0} are allowed to vary with the spanwise coordinate to account for geometric and aerodynamic twist, such as the examples shown in Fig. 2. For a given wing design, at a given angle of attack and airspeed, the planform shape, airfoil section lift slope, geometric angle of attack, and zero-lift angle of attack are all known functions of spanwise position. The only unknown in Eq. (2) is the section circulation distribution $\Gamma(z)$.

An analytical solution to Prandtl's lifting-line equation can be obtained in terms of a Fourier sine series. From this solution the circulation distribution is given by

$$\Gamma(\theta) = 2bV_\infty \sum_{n=1}^{\infty} A_n \sin(n\theta) \tag{3}$$

where

$$\theta = \cos^{-1}(-2z/b) \tag{4}$$

and the Fourier coefficients A_n must satisfy the relation

$$\sum_{n=1}^{\infty} A_n\left[1 + n\frac{\tilde{C}_{L,\alpha}c(\theta)}{4b\sin(\theta)}\right]\sin(n\theta) = \frac{\tilde{C}_{L,\alpha}c(\theta)[\alpha(\theta) - \alpha_{L0}(\theta)]}{4b} \tag{5}$$

From this circulation distribution, the resulting lift and induced-drag coefficients for the finite wing are found to be

$$C_L = \pi R_A A_1 \tag{6}$$

$$C_{Di} = \pi R_A \sum_{n=1}^{\infty} nA_n^2 = \frac{C_L^2}{\pi R_A} + \pi R_A \sum_{n=2}^{\infty} nA_n^2 \tag{7}$$

Received 26 November 2002; presented as Paper 2003-0393 at the 41st Aerospace Sciences Meeting, Reno, NV, 6–9 January 2003; revision received 19 February 2003; accepted for publication 26 May 2003.

*Professor, Mechanical and Aerospace Engineering Department, 4130 Old Main Hill. Member AIAA.

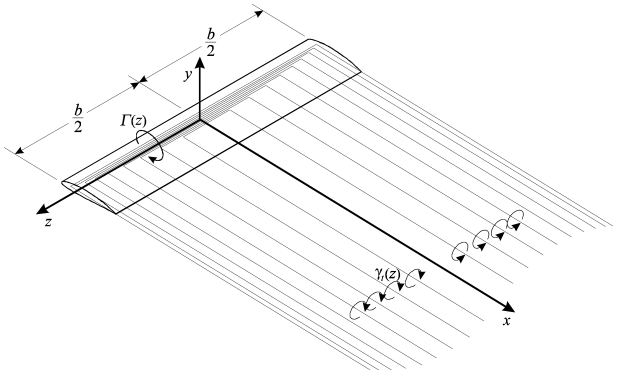

Fig. 1 Prandtl's model for the bound vorticity and trailing vortex sheet generated by a finite wing.

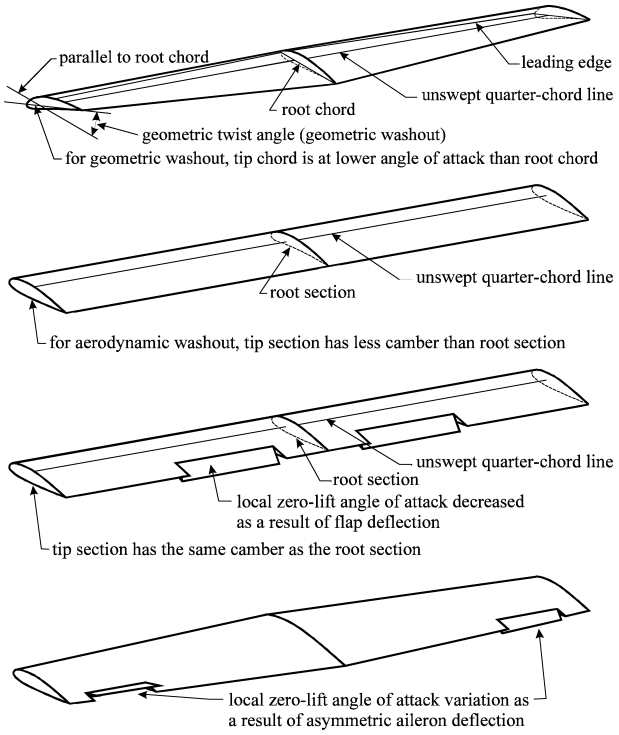

Fig. 2 Examples of geometric and aerodynamic twist.

Historically, the coefficients in this infinite series solution have usually been evaluated from collocation methods. Typically, the series is truncated to a finite number of terms and the coefficients in the finite series are evaluated by requiring Eq. (5) to be satisfied at a number of spanwise locations equal to the number of terms in the series. A very straightforward method was first published by Glauert.[3] The most popular method, based on Gaussian quadrature, was originally developed by Multhopp.[4] Most recently, Rasmussen and Smith[5] presented a more rigorous and rapidly converging method, based on a Fourier series expansion similar to that first presented by Lotz[6] and described by Karamcheti.[7]

The general lifting-line solution expressed in the form of Eqs. (3–7) is cumbersome for evaluating traditional wing properties, because the Fourier coefficients depend on angle of attack and must be reevaluated for each operating point studied. For a wing with no geometric or aerodynamic twist, α and α_{L0} are independent of θ and the Fourier coefficients in Eq. (5) can be written as[3]

$$A_n \equiv a_n(\alpha - \alpha_{L0}) \tag{8}$$

which reduces Eq. (5) to

$$\sum_{n=1}^{\infty} a_n \left[\frac{4b}{\tilde{C}_{L,\alpha} c(\theta)} + \frac{n}{\sin(\theta)} \right] \sin(n\theta) = 1 \tag{9}$$

The Fourier coefficients obtained from Eq. (9) are independent of the angle of attack and only depend on the airfoil section lift slope and wing planform. Using Eq. (8) in Eqs. (6) and (7), the lift and induced-drag coefficients for a wing with no geometric or aerodynamic twist can be written as follows:

$$C_L = \frac{\tilde{C}_{L,\alpha}(\alpha - \alpha_{L0})}{(1 + \tilde{C}_{L,\alpha}/\pi R_A)(1 + \kappa_L)} \tag{10}$$

$$C_{Di} = \frac{C_L^2(1 + \kappa_D)}{\pi R_A} \tag{11}$$

where

$$\kappa_L = \frac{1 - (1 + \pi R_A/\tilde{C}_{L,\alpha})a_1}{(1 + \pi R_A/\tilde{C}_{L,\alpha})a_1} \tag{12}$$

$$\kappa_D = \sum_{n=2}^{\infty} n \left(\frac{a_n}{a_1} \right)^2 \tag{13}$$

For a detailed presentation of Prandtl's lifting-line theory see Refs. 8–12.

Solution for Wings with Geometric and Aerodynamic Twist

For a wing with geometric and/or aerodynamic twist, the aerodynamic angle of attack, $\alpha - \alpha_{L0}$, is not constant along the span and the relation given by Eq. (8) cannot be applied. Because geometric and aerodynamic twist enter the lifting-line formulation only as a sum, we need not distinguish between these two types of twist. To avoid repeated use of the lengthy and cumbersome phrase geometric and aerodynamic twist, in the following presentation the words twist and washout will be used synonymously to indicate a spanwise variation in either the local geometric angle of attack or the local zero-lift angle of attack. Washout is treated as positive at those sections with a lower aerodynamic angle of attack than the root, and negative at those sections with a higher aerodynamic angle of attack than the root.

The procedure commonly used for lifting-line analysis of twisted wings is based on Eqs. (3–7) and requires evaluating separate sets of the Fourier coefficients A_n for more than one angle of attack. Because the unstalled lift coefficient is a linear function of angle of attack, the wing lift slope and zero-lift angle of attack for a finite twisted wing can be determined by evaluating only two sets of coefficients A_n, one set for each of two different angles of attack. However, as pointed out by Karamcheti,[7] the induced-drag coefficient for a twisted wing is not a linear function of the lift coefficient squared, as it is for an untwisted wing. Thus, to obtain the induced-drag polar for a twisted wing using this procedure, several sets of the Fourier coefficients A_n are determined over a range of angles of attack. Bertin[9] as well as Kuethe and Chow[11] present the details of this procedure together with example computations.

Glauert[3] authored the first textbook to present a lifting-line analysis for twisted wings. In this work, he considered only the rectangular planform with a linear spanwise symmetric variation in washout. In the 1930s and 1940s this type of analysis became quite commonplace (see, for example, Refs. 13–21). In addition to modeling a continuous variation in twist along the span of a finite wing, lifting-line theory has also been used to evaluate the spanwise lift distribution resulting from a step change in aerodynamic angle of attack, which is caused by the deflection of partial span trailing-edge flaps and ailerons.[22–28] Because a fairly large number of terms must be carried to adequately represent the Fourier expansion of a step function, lifting-line analysis for wings with deflected flaps and ailerons was extremely laborious prior to the development of the digital computer. This labor was amplified by the fact that the procedure required evaluating a complete set of Fourier coefficients for each angle for attack and flap deflection angle investigated.

A more practical form of the lifting-line solution for twisted wings can be obtained by using the simple change of variables

$$\alpha(\theta) - \alpha_{L0}(\theta) \equiv (\alpha - \alpha_{L0})_{\text{root}} - \Omega\omega(\theta) \tag{14}$$

where Ω is defined to be the maximum total washout, geometric plus aerodynamic,

$$\Omega \equiv (\alpha - \alpha_{L0})_{\text{root}} - (\alpha - \alpha_{L0})_{\max} \tag{15}$$

and $\omega(\theta)$ is the washout distribution normalized with respect to the maximum total washout:

$$\omega(\theta) \equiv \frac{\alpha(\theta) - \alpha_{L0}(\theta) - (\alpha - \alpha_{L0})_{\text{root}}}{(\alpha - \alpha_{L0})_{\max} - (\alpha - \alpha_{L0})_{\text{root}}} \tag{16}$$

The normalized washout distribution function $\omega(\theta)$ is independent of angle of attack and varies from 0.0 at the root to 1.0 at the point of maximum washout, commonly at the wingtips.

Using Eq. (14) in Eq. (15) gives

$$\sum_{n=1}^{\infty} A_n \left[1 + n\frac{\tilde{C}_{L,\alpha} c(\theta)}{4b \sin(\theta)} \right] \sin(n\theta)$$

$$= \frac{\tilde{C}_{L,\alpha} c(\theta)}{4b} [(\alpha - \alpha_{L0})_{\text{root}} - \Omega\omega(\theta)] \tag{17}$$

The Fourier coefficients A_n in Eq. (17) can be conveniently written as

$$A_n \equiv a_n(\alpha - \alpha_{L0})_{\text{root}} - b_n\Omega \tag{18}$$

where the Fourier coefficients a_n and b_n are obtained from

$$\sum_{n=1}^{\infty} a_n \left[\frac{4b}{\tilde{C}_{L,\alpha} c(\theta)} + \frac{n}{\sin(\theta)} \right] \sin(n\theta) = 1 \tag{19}$$

$$\sum_{n=1}^{\infty} b_n \left[\frac{4b}{\tilde{C}_{L,\alpha} c(\theta)} + \frac{n}{\sin(\theta)} \right] \sin(n\theta) = \omega(\theta) \tag{20}$$

Comparing Eq. (19) with Eq. (9), we see that the Fourier coefficients in Eq. (19) are those corresponding to the solution for a wing of the same planform shape but without washout. The solution to Eq. (20) can be obtained in a similar manner and is also independent of angle of attack.

Truncating the series, the first N Fourier coefficients b_n can be obtained by enforcing Eq. (20) at N different spanwise cross sections of the wing. With the first and last sections located at the wingtips and the intermediate sections spaced equally in θ, this gives the following system of equations:

$$\sum_{n=1}^{N} b_n \left[\frac{4b}{\tilde{C}_{L,\alpha} c(\theta_i)} + \frac{n}{\sin(\theta_i)} \right] \sin(n\theta_i) = \omega(\theta_i)$$

$$\theta_i = \frac{(i-1)\pi}{N-1}, \qquad i = 1, N$$

After applying the following relations at the wingtips, $\theta = 0$ and $\theta = \pi$,

$$\left[\frac{\sin(n\theta)}{\sin(\theta)} \right]_{\theta \to 0} = n$$

$$\left[\frac{\sin(n\theta)}{\sin(\theta)} \right]_{\theta \to \pi} = (-1)^{n+1} n$$

we have

$$\sum_{n=1}^{N} b_n n^2 = \omega(0)$$

$$\sum_{n=1}^{N} b_n \left[\frac{4b}{\tilde{C}_{L,\alpha} c(\theta_i)} + \frac{n}{\sin(\theta_i)} \right] \sin(n\theta_i) = \omega(\theta_i)$$

$$\theta_i = \frac{(i-1)\pi}{N-1}, \qquad i = 2, N-1$$

$$\sum_{n=1}^{N} b_n (-1)^{n+1} n^2 = \omega(\pi) \tag{21}$$

This $N \times N$ system is readily solved for the N Fourier coefficients b_n. It should be noted that the matrix obtained for the coefficients of b_n on the left-hand side of Eq. (21) is exactly the same as that obtained from Eq. (19) for determination of the Fourier coefficients a_n. Thus, this matrix needs to be inverted only once. To obtain the planform Fourier coefficients a_n, the $N \times N$ inverted matrix is multiplied by an N component column vector with all components set to 1. Multiplying the same $N \times N$ inverted matrix by an N component column vector obtained from the washout distribution function yields the Fourier coefficients b_n. If both the wing planform and washout distribution function are spanwise symmetric, all of the even Fourier coefficients in both a_n and b_n will be zero. However, carrying both the odd and even Fourier coefficients and distributing the collocation points over both sides of the wing allows for the analysis of asymmetric twist, such as that produced by aileron deflection. With modern tools, the added computational burden is insignificant.

Other methods of evaluating the Fourier coefficients[5,6] could also be used. As was shown by Bertin,[9] the different methods give similar accuracy for a given truncation level and produce identical results when the number of terms carried from the infinite series becomes large. The results obtained from the present analysis do not depend on the method used to evaluate the Fourier coefficients, provided that a sufficient number of terms are carried. With today's technology, 100 to 1000 terms in the infinite series can be evaluated as fast as the result can be written to the screen. Thus, carrying more terms in the Fourier series is the easiest way to improve accuracy.

Using Eq. (18) in Eq. (7), the lift coefficient for a wing with washout can be expressed as

$$C_L = \pi R_A A_1 = \pi R_A [a_1(\alpha - \alpha_{L0})_{\text{root}} - b_1\Omega] \tag{22}$$

Using Eq. (18) in Eq. (7), the induced-drag coefficient is given by

$$C_{Di} = \pi R_A \sum_{n=1}^{\infty} n A_n^2 = \pi R_A [a_1(\alpha - \alpha_{L0})_{\text{root}} - b_1\Omega]^2$$

$$+ \pi R_A \sum_{n=2}^{\infty} n[a_n(\alpha - \alpha_{L0})_{\text{root}} - b_n\Omega]^2$$

or, in view of Eq. (22),

$$C_{Di} = \frac{C_L^2}{\pi R_A} + \pi R_A \sum_{n=2}^{\infty} n\left[a_n^2(\alpha - \alpha_{L0})_{\text{root}}^2 \right.$$

$$\left. - 2a_n b_n(\alpha - \alpha_{L0})_{\text{root}}\Omega + b_n^2\Omega^2 \right] \tag{23}$$

Equations (22) and (23) can be algebraically rearranged to yield

$$C_L = C_{L,\alpha}[(\alpha - \alpha_{L0})_{\text{root}} - \varepsilon_\Omega\Omega] \tag{24}$$

$$C_{Di} = \frac{C_L^2(1 + \kappa_D) - \kappa_{DL} C_L C_{L,\alpha}\Omega + \kappa_{D\Omega}(C_{L,\alpha}\Omega)^2}{\pi R_A} \tag{25}$$

where

$$C_{L,\alpha} = \pi R_A a_1 = \frac{\tilde{C}_{L,\alpha}}{(1 + \tilde{C}_{L,\alpha}/\pi R_A)(1 + \kappa_L)} \tag{26}$$

$$\kappa_L \equiv \frac{1 - (1 + \pi R_A/\tilde{C}_{L,\alpha})a_1}{(1 + \pi R_A/\tilde{C}_{L,\alpha})a_1} \tag{27}$$

$$\varepsilon_\Omega \equiv \frac{b_1}{a_1} \tag{28}$$

$$\kappa_D \equiv \sum_{n=2}^{\infty} n \frac{a_n^2}{a_1^2} \tag{29}$$

$$\kappa_{DL} \equiv 2\frac{b_1}{a_1} \sum_{n=2}^{\infty} n \frac{a_n}{a_1} \left(\frac{b_n}{b_1} - \frac{a_n}{a_1} \right) \tag{30}$$

$$\kappa_{D\Omega} \equiv \left(\frac{b_1}{a_1} \right)^2 \sum_{n=2}^{\infty} n \left(\frac{b_n}{b_1} - \frac{a_n}{a_1} \right)^2 \tag{31}$$

Comparing Eqs. (24–31) with Eqs. (10–13), we see that washout increases the zero-lift angle of attack for any wing. However, the lift slope for a wing of arbitrary planform shape is not affected by washout. Equations (24), (26), and (27) show that the lift slope for a twisted finite wing depends only on the airfoil section lift slope, the wing aspect ratio, and the first Fourier coefficient in the infinite series obtained from Eq. (19). From examination of Eq. (19), it is seen that the Fourier coefficients a_n depend only on wing planform and airfoil section lift slope. No approximation was made in the development of these equations beyond those that are already included in Eq. (2), which is the foundation for all lifting-line theory. Thus, lifting-line theory will always predict that the lift slope for an unstalled finite wing is independent of geometric and aerodynamic twist.

Also notice that the induced drag for a wing with washout is not zero at the angle of attack for which the wing develops zero net lift. In addition to the usual component of induced drag, which is proportional to the lift coefficient squared, a wing with washout produces a component of induced drag that is proportional to the washout squared and this gives rise to induced drag at zero net lift. There is also a component of induced drag that varies with the product of the lift coefficient and the washout. The induced drag, which is produced on a twisted wing at zero net lift, still results from the production of lift on the wing. For a wing with geometric or aerodynamic twist, there is no global angle of attack for which the wing carries zero lift over all segments of its span. When the net lift on a twisted wing is zero, some spanwise segments of the wing are carrying positive lift while other spanwise segments are carrying negative lift. Induced drag is generated as a result of the production of this lift, even though the negative lift exactly balances the positive lift so that no net lift is generated by the wing.

Elliptic Wings with Linear Washout

An elliptic wing with no geometric or aerodynamic twist provides a planform shape that produces minimum possible induced drag for a given lift coefficient and aspect ratio. The chord of an elliptic wing varies with the spanwise coordinate according to the relation

$$c(z) = (4b/\pi R_A)\sqrt{1 - (2z/b)^2}$$

or

$$c(\theta) = (4b/\pi R_A)\sin(\theta) \tag{32}$$

Using Eq. (32) in Eqs. (19) and (20) yields

$$\sum_{n=1}^{\infty} a_n \left(\frac{\pi R_A}{\tilde{C}_{L,\alpha}} + n \right) \sin(n\theta) = \sin(\theta) \tag{33}$$

$$\sum_{n=1}^{\infty} b_n \left(\frac{\pi R_A}{\tilde{C}_{L,\alpha}} + n \right) \sin(n\theta) = \omega(\theta)\sin(\theta) \tag{34}$$

The well-known solution to Eq. (33) is

$$a_1 = \frac{\tilde{C}_{L,\alpha}}{\pi R_A + \tilde{C}_{L,\alpha}}, \qquad a_n = 0, \qquad n \neq 1 \tag{35}$$

and the solution to Eq. (34) is given by the Fourier integral

$$b_n = \frac{2}{\pi} \left(\frac{\tilde{C}_{L,\alpha}}{\pi R_A + n\tilde{C}_{L,\alpha}} \right) \int_0^{\pi} \omega(\theta)\sin(\theta)\sin(n\theta)\,\mathrm{d}\theta \tag{36}$$

For the case of linear washout, the normalized washout distribution function is

$$\omega(z) = |2z/b| \qquad \text{or} \qquad \omega(\theta) = |\cos(\theta)| \tag{37}$$

Using Eq. (37) in Eq. (36) and applying the trigonometric identity $\sin(2\theta) = 2\sin(\theta)\cos(\theta)$ yields

$$b_n = \frac{1}{\pi} \left(\frac{\tilde{C}_{L,\alpha}}{\pi R_A + n\tilde{C}_{L,\alpha}} \right) \left[\int_0^{\pi/2} \sin(2\theta)\sin(n\theta)\,\mathrm{d}\theta - \int_{\pi/2}^{\pi} \sin(2\theta)\sin(n\theta)\,\mathrm{d}\theta \right] \tag{38}$$

The integrals on the right-hand side of Eq. (38) can be evaluated from

$$\int \sin(m\theta)\sin(n\theta)\,\mathrm{d}\theta = \begin{cases} \dfrac{\sin[(n-m)\theta]}{2(n-m)} - \dfrac{\sin[(n+m)\theta]}{2(n+m)}, & n \neq m \\ \dfrac{\theta}{2} - \dfrac{\sin(2n\theta)}{4n}, & n = m \end{cases}$$

which yields

$$b_n = \frac{1}{\pi} \left(\frac{\tilde{C}_{L,\alpha}}{\pi R_A + n\tilde{C}_{L,\alpha}} \right) \begin{cases} \dfrac{4\sin(n\pi/2)}{4 - n^2}, & n \neq 2 \\ 0, & n = 2 \end{cases} \tag{39}$$

Using Eqs. (35) and (39) in Eqs. (27–31) gives

$$\kappa_L = 0, \qquad \varepsilon_\Omega = (4/3\pi), \qquad \kappa_D = 0, \qquad \kappa_{DL} = 0$$

$$\kappa_{D\Omega} = \sum_{n=3}^{\infty} n \left[\frac{1}{\pi} \left(\frac{\pi R_A + \tilde{C}_{L,\alpha}}{\pi R_A + n\tilde{C}_{L,\alpha}} \right) \frac{4\sin(n\pi/2)}{4 - n^2} \right]^2$$

Using these results in Eqs. (24) and (25), together with the relation

$$\sin^2\left(\frac{n\pi}{2}\right) = \begin{cases} 1, & \text{for } n \text{ odd} \\ 0, & \text{for } n \text{ even} \end{cases}$$

the lift and induced-drag coefficients for an elliptic wing with linear washout are given by

$$C_L = C_{L,\alpha} \left[(\alpha - \alpha_{L0})_{\text{root}} - \frac{4}{3\pi}\Omega \right]$$

$$C_{L,\alpha} = \frac{\tilde{C}_{L,\alpha}}{1 + \tilde{C}_{L,\alpha}/\pi R_A} \tag{40}$$

$$C_{Di} = \frac{C_L^2 + \kappa_{D\Omega}(C_{L,\alpha}\Omega)^2}{\pi R_A}$$

$$\kappa_{D\Omega} = \sum_{i=1}^{\infty} \frac{16(2i+1)}{[(2i+1)^2 - 4]^2\pi^2} \left(\frac{\pi R_A + \tilde{C}_{L,\alpha}}{\pi R_A + (2i+1)\tilde{C}_{L,\alpha}} \right)^2 \tag{41}$$

From Eq. (41) it can be seen that linear washout always increases induced drag for an elliptic wing. The variation of $\kappa_{D\Omega}$ with aspect ratio for an elliptic planform with linear washout and a section lift slope of 2π is shown in Fig. 3. This solution is consistent with the results presented by Filotas.[29]

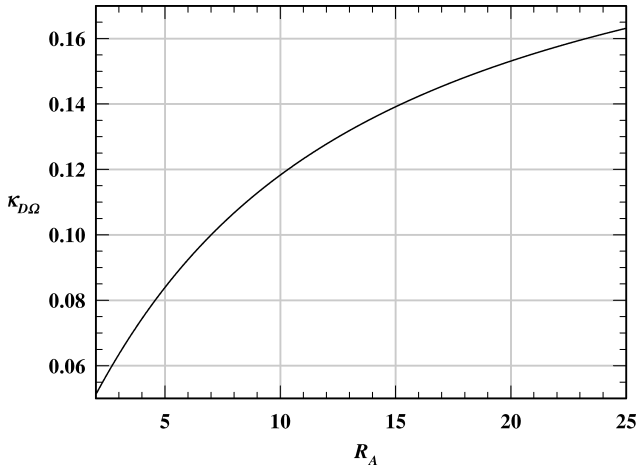

Fig. 3 Washout contribution to the induced-drag factor for elliptic wings with linear washout.

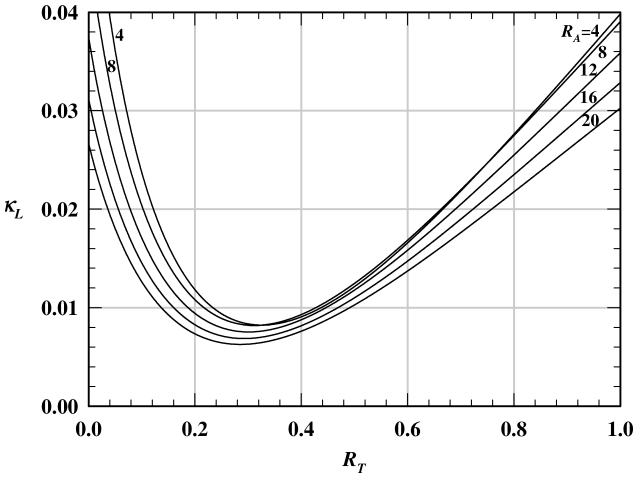

Fig. 4 The lift slope factor for tapered wings.

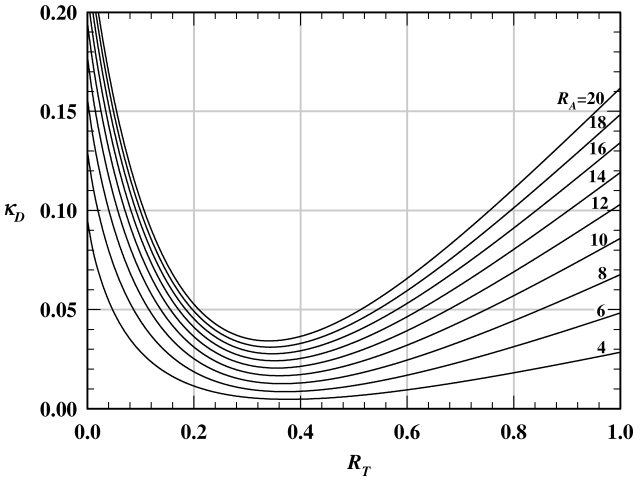

Fig. 5 Planform contribution to the induced-drag factor for tapered wings.

Tapered Wings with Linear Washout

Whereas elliptic wings with no geometric or aerodynamic twist produce minimum possible induced drag, they are more expensive to manufacture than simple rectangular wings. The tapered wing has commonly been used as a compromise. A tapered wing has a chord that varies linearly with the spanwise coordinate according to the following relation:

$$c(z) = \frac{2b}{R_A(1+R_T)}[1-(1-R_T)|2z/b|]$$

or

$$c(\theta) = \frac{2b}{R_A(1+R_T)}[1-(1-R_T)|\cos(\theta)|] \tag{42}$$

Using Eqs. (37) and (42) in Eqs. (19) and (20) yields the results for a tapered wing with linear washout:

$$\sum_{n=1}^{\infty} a_n \left\{ \frac{2R_A(1+R_T)}{\tilde{C}_{L,\alpha}[1-(1-R_T)|\cos(\theta)|]} + \frac{n}{\sin(\theta)} \right\} \sin(n\theta) = 1 \tag{43}$$

$$\sum_{n=1}^{\infty} b_n \left\{ \frac{2R_A(1+R_T)}{\tilde{C}_{L,\alpha}[1-(1-R_T)|\cos(\theta)|]} + \frac{n}{\sin(\theta)} \right\} \sin(n\theta) = |\cos(\theta)| \tag{44}$$

The solution obtained from Eq. (43) for the Fourier coefficients a_n is commonly used for predicting the lift and induced-drag coefficients for a tapered wing with no geometric or aerodynamic twist. This solution is discussed in most engineering textbooks on aerodynamics.[8–12] Figures 4 and 5 show how the lift slope and induced-drag factors vary with aspect ratio and taper ratio for tapered wings with no geometric or aerodynamic twist. In these and all following figures an airfoil section lift slope of 2π was used. The results shown in Fig. 5 have sometimes led to the conclusion that a tapered wing with a taper ratio of about 0.4 always produces less induced drag than a rectangular wing of the same aspect ratio developing the same lift. As a result, tapered wings are commonly used as a means of reducing induced drag. However, this reduction in drag comes at a price. Because a tapered wing has a lower Reynolds number at the wingtips than at the root, a tapered wing with no geometric or aerodynamic twist tends to stall first in the region near the wingtips. This wingtip stall can lead to poor handling characteristics during stall recovery.

When interpreting the results shown in Fig. 5, it has proven easy to lose sight of the fact that these results can be used to predict total induced drag only for the special case of wings with no geometric or aerodynamic twist. This is only one of many possible washout distributions that could be used for a wing of any given planform. Furthermore, it is not the washout distribution that produces minimum induced drag with finite lift, except for the special case of an elliptic planform. When the effects of washout are included, it can be shown that the conclusions sometimes reached from consideration of only those results shown in Fig. 5 are erroneous.

The induced-drag coefficient for a wing with washout can be predicted from Eq. (25) with the definitions given in Eqs. (29–31). For tapered wings with linear washout, the Fourier coefficients b_n can be obtained from Eq. (44) in exactly the same manner as the coefficients a_n are obtained from Eq. (43). Using the Fourier coefficients so obtained in Eqs. (28), (30), and (31) produces the results shown in Figs. 6–8. Notice from either Eq. (31) or Fig. 8 that $\kappa_{D\Omega}$ is always positive. Thus, the third term in the numerator on the right-hand side of Eq. (25) always contributes to an increase in induced drag. However, from the results shown in Fig. 7, we see that the second term in the numerator on the right-hand side of Eq. (25) can either increase or decrease the induced drag, depending on the signs of κ_{DL} and Ω. This raises an important question regarding wing efficiency. What level and distribution of washout will result in minimum induced drag for a given wing planform and lift coefficient?

Minimizing Induced Drag with Washout

For a wing of any given planform shape with a fixed washout distribution function, the induced drag can be minimized with washout as a result of the tradeoff between the second and third terms in the numerator on the right-hand side of Eq. (25). Thus, Eq. (25) can be

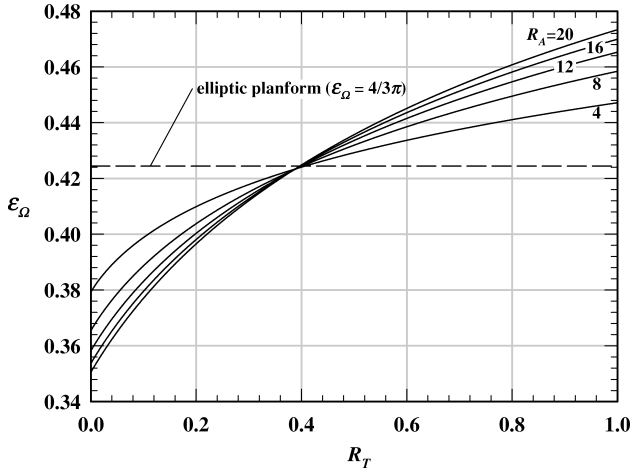

Fig. 6 Washout effectiveness for tapered wings with linear washout.

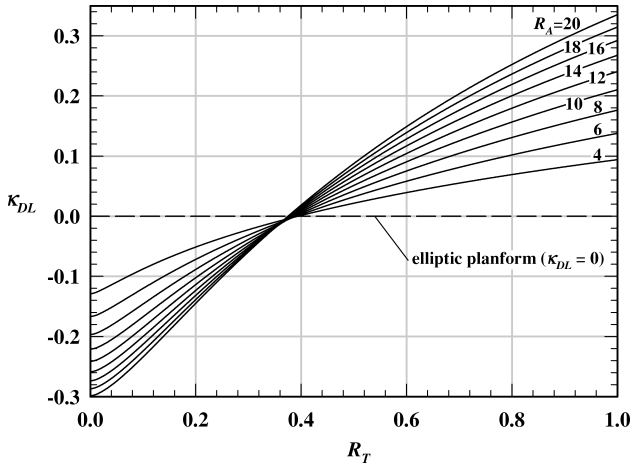

Fig. 7 Lift-washout contribution to the induced-drag factor for tapered wings with linear washout.

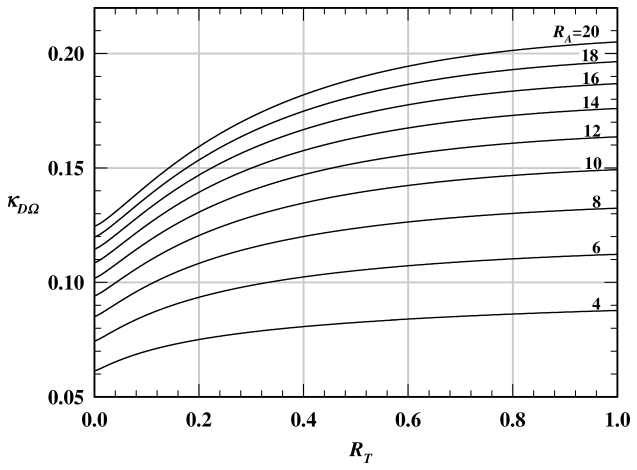

Fig. 8 Washout contribution to the induced-drag factor for tapered wings with linear washout.

used to determine the optimum value of total washout, which will result in minimum induced drag for any washout distribution and any specified lift coefficient. Differentiating Eq. (25) with respect to total washout at constant lift coefficient gives

$$\frac{\partial C_{Di}}{\partial \Omega} = \frac{-\kappa_{DL} C_L C_{L,\alpha} + 2\kappa_{D\Omega} C_{L,\alpha}^2 \Omega}{\pi R_A}$$

From this result it can be seen that minimum induced drag is attained for any given wing planform, $c(z)$, any given washout distribution, $\omega(z)$, and any given design lift coefficient, C_{Ld}, by using an optimum total washout, Ω_{opt} given by the relation

$$C_{L,\alpha}\Omega_{\text{opt}} = \frac{\kappa_{DL} C_{Ld}}{2\kappa_{D\Omega}} \tag{45}$$

Because κ_{DL} is zero for an elliptic wing, Eq. (45) shows that an elliptic wing is optimized with no washout. From consideration of Eq. (45), together with the results shown in Figs. 7 and 8, we see that tapered wings with linear washout and taper ratios greater than 0.4 are optimized with positive washout, whereas those with taper ratios less than about 0.4 produce minimum induced drag with negative washout. However, a taper ratio less than 0.4 with negative washout would result in very poor stall characteristics and would not be practical.

Using the value of optimum washout from Eq. (45) in the expression for induced-drag coefficient that is given by Eq. (25), we find that the induced-drag coefficient for a wing of arbitrary planform with a fixed washout distribution and optimum total washout is given by

$$(C_{Di})_{\text{opt}} = \frac{C_L^2}{\pi R_A}\left[1 + \kappa_D - \frac{\kappa_{DL}^2}{4\kappa_{D\Omega}}\left(2 - \frac{C_{Ld}}{C_L}\right)\frac{C_{Ld}}{C_L}\right] \tag{46}$$

From Eq. (46) it can be seen that a wing with optimum washout will always produce less induced drag than a wing with no washout having the same planform and aspect ratio, provided that the actual lift coefficient is greater than one-half the design lift coefficient. When the actual lift coefficient is equal to the design lift coefficient, the induced-drag coefficient for a wing with optimum washout is

$$(C_{Di})_{\text{opt}} = \left(C_L^2/\pi R_A\right)(1 + \kappa_{Do}), \qquad \kappa_{Do} \equiv \kappa_D - \left(\kappa_{DL}^2/4\kappa_{D\Omega}\right) \tag{47}$$

For tapered wings with linear washout, the variations in κ_{Do} with aspect ratio and taper ratio are shown in Fig. 9. For comparison, the dashed lines in this figure show the same results for wings with no washout. Notice that when linear washout is used to further optimize tapered wings, taper ratios in the range of 0.4 correspond closely to a maximum in induced drag, not to a minimum.

The choice of a linear washout distribution, which was used to generate the results shown in Fig. 9, is as arbitrary as the choice of no washout. Whereas a linear variation in washout is commonly used and simple to implement, it is not the optimum washout distribution for wings with linear taper. Minimum induced drag for a given finite lift coefficient occurs when the right-hand side of Eq. (5) varies with the spanwise coordinate in proportion to $\sin(\theta)$. This requires that the product of the local chord length and the local aerodynamic angle

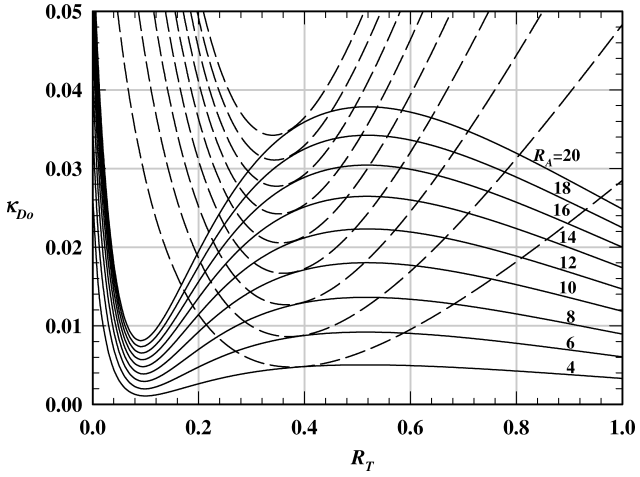

Fig. 9 Optimum induced-drag factor for tapered wings with linear washout.

of attack, $\alpha - \alpha_{L0}$, varies elliptically with the spanwise coordinate; that is,

$$\frac{c(z)[\alpha(z) - \alpha_{L0}(z)]}{\sqrt{1-(2z/b)^2}} = \frac{c(\theta)[\alpha(\theta) - \alpha_{L0}(\theta)]}{\sin(\theta)} = \text{Const} \qquad (48)$$

There are many possibilities for wing geometry that will satisfy this condition. The elliptic planform with no geometric or aerodynamic twist is only one such geometry. Because the local aerodynamic angle of attack decreases along the span in direct proportion to the increase in washout, Eq. (48) can only be satisfied if the washout distribution satisfies the following relation:

$$\frac{c(z)[1 - \omega(z)]}{\sqrt{1-(2z/b)^2}} = \frac{c(\theta)[1 - \omega(\theta)]}{\sin(\theta)} = \text{Const} \qquad (49)$$

Equation (49) is satisfied by the spanwise washout distribution

$$\omega(z) = 1 - \frac{\sqrt{1-(2z/b)^2}}{c(z)/c_{\text{root}}} \quad \text{or} \quad \omega(\theta) = 1 - \frac{\sin(\theta)}{c(\theta)/c_{\text{root}}} \qquad (50)$$

For wings with linear taper, this gives

$$\omega(z) = 1 - \frac{\sqrt{1-(2z/b)^2}}{1-(1-R_T)|2z/b|}$$

or

$$\omega(\theta) = 1 - \frac{\sin(\theta)}{1-(1-R_T)|\cos(\theta)|} \qquad (51)$$

This washout distribution is shown in Fig. 10 for several values of taper ratio. Results obtained for tapered wings with this washout distribution are presented in Figs. 11–13.

When an unswept wing of arbitrary planform has the washout distribution specified by Eq. (50), the value of κ_{Do} as defined in Eq. (47) is always identically zero. With this spanwise washout distribution and the total washout set according to Eq. (45), an unswept wing of any planform shape can be designed to operate at a given lift coefficient with the same minimum induced drag as that produced by an untwisted elliptic wing with the same aspect ratio and lift coefficient. This optimum spanwise washout distribution produces an elliptic spanwise lift distribution, which always results in uniform downwash over the wingspan and minimum possible induced drag. For example, a rectangular wing requires an elliptic washout distribution according to Eq. (51). With this washout distribution, an aspect ratio of 8.0, and a section lift slope of 2π, Eqs. (29–31) and (47) give

$$\kappa_D = 0.0676113, \qquad \kappa_{DL} = 0.1379367$$

$$\kappa_{D\Omega} = 0.0703526, \qquad \kappa_{Do} = 0.0000000$$

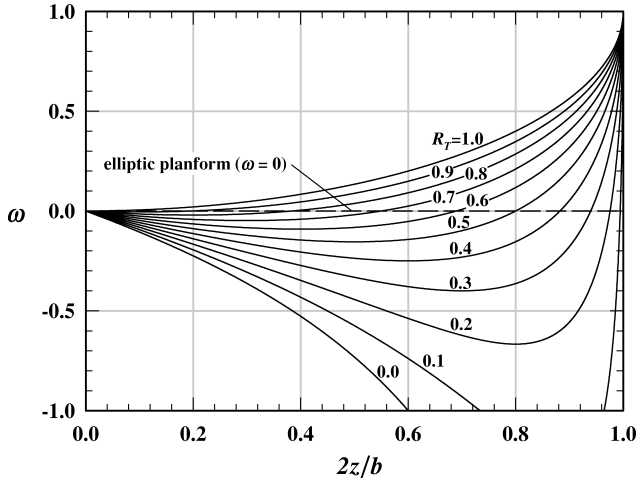

Fig. 10 Optimum washout distribution for wings with linear taper.

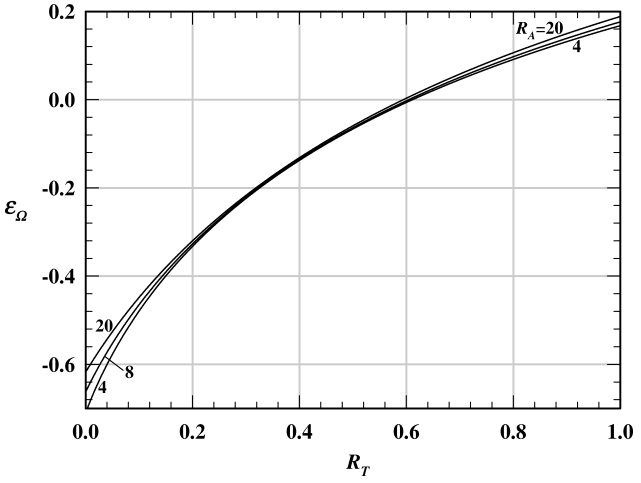

Fig. 11 Washout effectiveness for tapered wings with optimum washout distribution.

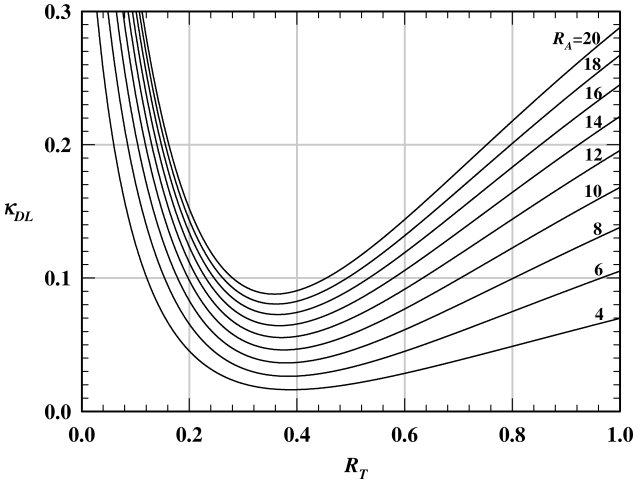

Fig. 12 Lift-washout contribution to the induced-drag factor for tapered wings with optimum washout distribution.

Similarly, a tapered wing of aspect ratio 8.0 and taper ratio 0.5 results in

$$\kappa_D = 0.0171896, \qquad \kappa_{DL} = 0.0455690$$

$$\kappa_{D\Omega} = 0.0302003, \qquad \kappa_{Do} = 0.0000000$$

These results were obtained by carrying a total of 99 terms in the infinite series, that is, 50 of the nonzero odd terms.

Consider an unswept wing with linear taper having the washout distribution given by Eq. (51). Using Eqs. (42) and (51) in Eqs. (19) and (20) yields

$$\sum_{n=1}^{\infty} \frac{a_n}{a_1} \sin(n\theta) + \frac{\tilde{C}_{L,\alpha}[1-(1-R_T)|\cos(\theta)|]}{2R_A(1+R_T)} \sum_{n=1}^{\infty} n \frac{a_n}{a_1} \frac{\sin(n\theta)}{\sin(\theta)}$$

$$= \frac{\tilde{C}_{L,\alpha}[1-(1-R_T)|\cos(\theta)|]}{2a_1 R_A(1+R_T)} \qquad (52)$$

$$\sum_{n=1}^{\infty} \frac{b_n}{b_1} \sin(n\theta) + \frac{\tilde{C}_{L,\alpha}[1-(1-R_T)|\cos(\theta)|]}{2R_A(1+R_T)} \sum_{n=1}^{\infty} n \frac{b_n}{b_1} \frac{\sin(n\theta)}{\sin(\theta)}$$

$$= \frac{\tilde{C}_{L,\alpha}[1-\sin(\theta)-(1-R_T)|\cos(\theta)|]}{2b_1 R_A(1+R_T)} \qquad (53)$$

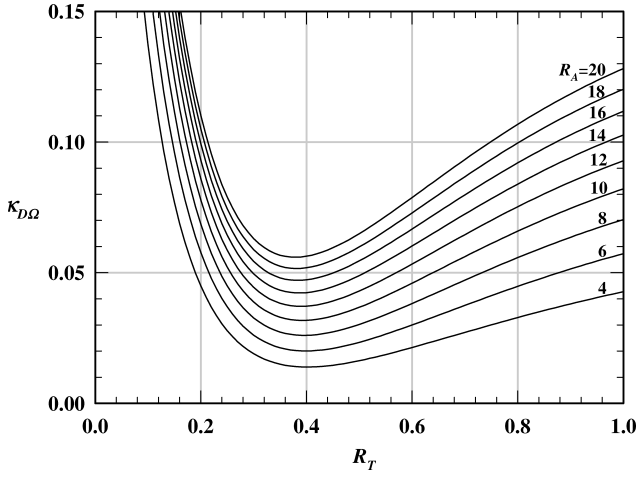

Fig. 13 Washout contribution to the induced-drag factor for tapered wings with optimum washout distribution.

To evaluate the induced drag for this wing we make use of the Fourier expansions,

$$1 = \frac{2}{\pi}\left[2\sin(\theta) + \sum_{m=1}^{\infty} \frac{2}{2m+1}\sin[(2m+1)\theta]\right] \tag{54}$$

$$|\cos(\theta)| = \frac{2}{\pi}\left[\sin(\theta) + \sum_{m=1}^{\infty} \frac{2m+1-(-1)^m}{2m(m+1)}\sin[(2m+1)\theta]\right] \tag{55}$$

and the trigonometric identities,

$$\frac{\sin[(2m+1)\theta]}{\sin(\theta)} = \frac{\sin[(2m-1)\theta]}{\sin(\theta)} + 2\cos(2m\theta) \tag{56}$$

$$2\cos(2m\theta)\sin[(2n+1)\theta] = \sin[(2m+2n+1)\theta] - \sin[(2m-2n-1)\theta] \tag{57}$$

Using Eqs. (54) through (57) in Eqs. (52) and (53), the Fourier coefficients, b_n, can be related to the Fourier coefficients, a_n. The result is

$$b_n = \begin{cases} a_1 - (1-a_1)\dfrac{\tilde{C}_{L,\alpha}}{2(1+R_T)R_A}, & \text{for } n = 1 \\ a_n\left[1 + \dfrac{\tilde{C}_{L,\alpha}}{2(1+R_T)R_A}\right], & \text{for } n \neq 1 \end{cases} \tag{58}$$

Applying Eq. (58) together with Eqs. (26) and (29) to Eqs. (30) and (31), we find that a wing with linear taper and the washout distribution specified by Eq. (51) results in

$$\kappa_{DL} = \frac{\pi\tilde{C}_{L,\alpha}}{(1+R_T)C_{L,\alpha}}\kappa_D \tag{59}$$

$$\kappa_{D\Omega} = \left(\frac{\pi\tilde{C}_{L,\alpha}}{2(1+R_T)C_{L,\alpha}}\right)^2\kappa_D \tag{60}$$

Using Eqs. (59) and (60) in Eq. (25), the induced drag for a wing with linear taper and the optimum washout distribution defined by Eq. (51) can be written as

$$C_{Di} = \frac{C_L^2}{\pi R_A} + \frac{\kappa_D}{\pi R_A}\left[C_L - \frac{\pi\tilde{C}_{L,\alpha}\Omega}{2(1+R_T)}\right]^2 \tag{61}$$

From Eq. (61), we see that any wing with linear taper and the corresponding optimum washout distribution specified by Eq. (51) produces the same minimum induced drag as an elliptic wing with no twist, provided that the total washout is related to the lift coefficient according to

$$\Omega_{\text{opt}} = \frac{2(1+R_T)C_L}{\pi\tilde{C}_{L,\alpha}} \tag{62}$$

A wing of arbitrary planform with an optimum washout distribution produces exactly the same induced drag as an elliptic wing with no washout, only while operating at the design lift coefficient. Whereas an elliptic wing produces minimum possible induced drag at all angles of attack, a washout-optimized wing of any other planform will produce minimum possible induced drag only at the angle of attack resulting in the design lift coefficient. However, a washout-optimized wing of nonelliptic planform very nearly duplicates the performance of an elliptic wing over a wide range of lift coefficients. This is demonstrated in Fig. 14 by comparing the induced drag generated by washout-optimized rectangular and tapered wings with that produced by an untwisted elliptic wing. Each of the three wings used for this figure has an aspect ratio of 8.0 and the rectangular and tapered wings are both optimized for a design lift coefficient of 0.4. The rectangular wing requires an elliptic washout distribution with 4.64 deg of total washout at the wingtips. The tapered wing has a taper ratio of 0.4 and uses the corresponding washout distribution shown in Fig. 10, which has 3.25 deg of total washout at the wingtips and maximum washin of 0.81 deg located at approximately 60% of

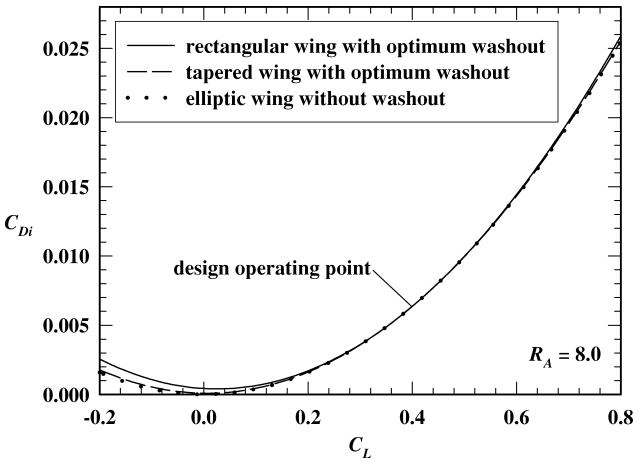

Fig. 14 Comparison of the induced drag produced by three wings of aspect ratio 8.0; a rectangular wing and a tapered wing (R_T = 0.4), both of which are washout-optimized for a design lift coefficient of 0.4, and an elliptic wing without washout.

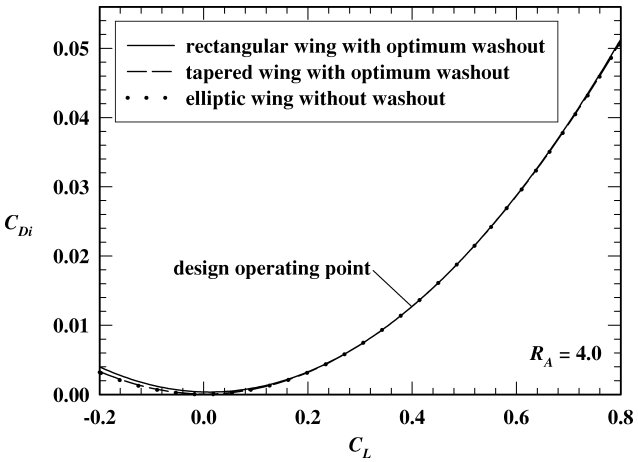

Fig. 15 Comparison of the induced drag produced by three wings of aspect ratio 4.0; a rectangular wing and a tapered wing (R_T = 0.4), both of which are washout-optimized for a design lift coefficient of 0.4, and an elliptic wing without washout.

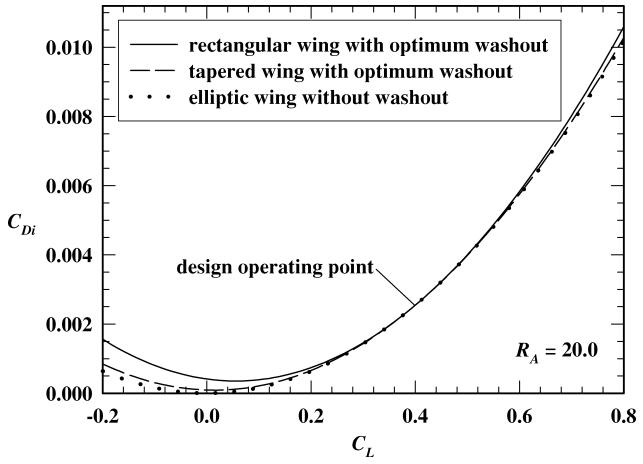

Fig. 16 Comparison of the induced drag produced by three wings of aspect ratio 20.0; a rectangular wing and a tapered wing ($R_T = 0.4$), both of which are washout-optimized for a design lift coefficient of 0.4, and an elliptic wing without washout.

the semispan. Similar results for wings of aspect ratio 4.0 and 20.0 are shown in Figs. 15 and 16.

Conclusions

When the traditional form of the lifting-line solution is used for wings with washout, the Fourier coefficients in the infinite series all depend on angle of attack. Because these coefficients must be reevaluated for each operating point, this form of the solution is cumbersome for evaluating traditional wing properties. A more practical form of the lifting-line solution for finite twisted wings has been presented here. This analytical solution is based on a change of variables that allows the infinite series to be divided into two parts, one series that depends only on planform and another series that depends on both planform and washout. The Fourier coefficients in both of these infinite series depend only on wing geometry and can be evaluated independent of the angle of attack.

The present form of the lifting-line solution for twisted wings shows that a wing of any planform shape can be optimized for any given design lift coefficient to produce exactly the same induced drag as an elliptic wing with no geometric or aerodynamic twist. The lifting-line theory predicts that minimum possible induced drag occurs whenever the product of local chord length and local aerodynamic angle of attack varies elliptically with the spanwise coordinate. The traditional solution to satisfying this requirement is the classic elliptic wing, which has a chord length that varies elliptically with the spanwise coordinate and constant aerodynamic angle of attack. However, this is only one of many possibilities for wing geometry that will satisfy the requirement for minimum possible induced drag. Another obvious solution is a wing with constant chord having a washout distribution that produces an elliptic variation in aerodynamic angle of attack. By using the more general washout distribution described in Eq. (50), together with the optimum total washout specified by Eq. (45), a wing of any planform can be made to satisfy the requirement for minimum possible induced drag.

Minimizing induced drag using both chord length and washout variation provides greater flexibility than using chord-length variation alone. For example, the stall characteristics of a wing depend on both the planform shape and the washout distribution. By using the optimum washout distribution, minimum induced drag can be maintained at the design lift coefficient for any planform shape. Thus, an additional degree-of-freedom is provided that can be used to help control the stall characteristics or any other measure of performance that is affected by wing planform and/or washout distribution.

From the results presented here, it can be seen that a wing of any planform shape having no geometric or aerodynamic twist is a special case of a washout-optimized wing. Except for the case of an elliptic planform, a wing with no washout is optimized for a design lift coefficient of zero. With the wing operating at any other lift coefficient, washout could be used to reduce the induced drag at low Mach numbers.

References

[1]Prandtl, L., "Tragflügel Theorie," *Nachricten von der Gesellschaft der Wissenschaften zu Göttingen*, Ges-chäeftliche Mitteilungen, Klasse, Germany, 1918, pp. 451–477.

[2]Prandtl, L., "Applications of Modern Hydrodynamics to Aeronautics," NACA TR-116, June 1921.

[3]Glauert, H., "The Monoplane Aerofoil," *The Elements of Aerofoil and Airscrew Theory*, Cambridge Univ. Press, Cambridge, UK, 1926, pp. 137–155.

[4]Multhopp, H., "Die Berechnung der Auftriebs Verteilung von Tragflugeln," *Luftfahrtforschung*, Vol. 15, No. 14, 1938, pp. 153–169.

[5]Rasmussen, M. L., and Smith, D. E., "Lifting-Line Theory for Arbitrarily Shaped Wings," *Journal of Aircraft*, Vol. 36, No. 2, 1999, pp. 340–348.

[6]Lotz, I., "Berechnung der Auftriebsverteilung beliebig geformter Flugel," *Zeitschrift für Flugtechnik und Motorluftschiffahrt*, Vol. 22, No. 7, 1931, pp. 189–195.

[7]Karamcheti, K., "Elements of Finite Wing Theory," *Ideal-Fluid Aerodynamics*, Wiley, New York, 1966, pp. 535–567.

[8]Anderson, J. D., "Incompressible Flow over Finite Wings: Prandtl's Classical Lifting-Line Theory," *Fundamentals of Aerodynamics*, 3rd ed., McGraw–Hill, New York, 2001, pp. 360–387.

[9]Bertin, J. J., "Incompressible Flow About Wings of Finite Span," *Aerodynamics for Engineers*, 4th ed., Prentice–Hall, Upper Saddle River, NJ, 2002, pp. 230–302.

[10]Katz, J., and Plotkin, A., "Finite Wing: The Lifting-Line Model," *Low-Speed Aerodynamics*, 2nd ed., Cambridge Univ. Press, Cambridge, UK, 2001, pp. 167–183.

[11]Kuethe, A. M., and Chow, C. Y., "The Finite Wing," *Foundations of Aerodynamics*, 5th ed., Wiley, New York, 1998, pp. 169–219.

[12]McCormick, B. W., "The Lifting-Line Model," *Aerodynamics, Aeronautics, and Flight Mechanics*, 2nd ed., Wiley, New York, 1995, pp. 112–119.

[13]Glauert, H., and Gates, S. B., "The Characteristics of a Tapered and Twisted Wing with Sweep-Back," *Reports and Memoranda 1226*, Aeronautical Research Council, London, Aug. 1929.

[14]Amstutz, E., "Calculation of Tapered Monoplane Wings," NACA TM-578, Feb. 1930.

[15]Anderson, R. F., "Charts for Determining the Pitching Moment of Tapered Wings with Sweepback and Twist," NACA TN-483, Dec. 1933.

[16]Anderson, R. F., "Determination of the Characteristics of Tapered Wings," NACA TR-572, May 1937.

[17]Datwiler, G., "Calculations of the Effect of Wing Twist on the Air Forces Acting on a Monoplane Wing," NACA TN-520, March 1935.

[18]Cohen, D., "A Method of Determining the Camber and Twist of a Surface to Support a Given Distribution of Lift," NACA TN-855, Aug. 1942.

[19]Falkner, V. M., "The Calculation of Aerodynamic Loading on Surfaces of Any Shape," *Reports and Memoranda 1910*, Aeronautical Research Council, London, Aug. 1943.

[20]DeYoung, J., and Harper, C. W., "Theoretical Symmetric Span Loading at Subsonic Speeds for Wings Having Arbitrary Plan Form," NACA TR-921, Dec. 1948.

[21]Stevens, V. I., "Theoretical Basic Span Loading Characteristics of Wings with Arbitrary Sweep, Aspect Ratio and Taper Ratio," NACA TN-1772, Dec. 1948.

[22]Munk, M. M., "On the Distribution of Lift Along the Span of an Airfoil with Displaced Ailerons," NACA TN-195, June 1924.

[23]Munk, M. M., "A New Relation Between the Induced Yawing Moment and the Rolling Moment of an Airfoil in Straight Motion," NACA TR-197, June 1925.

[24]Glauert, H., "Theoretical Relationships for an Airfoil with Hinged Flap," *Reports and Memoranda 1095*, Aeronautical Research Council, London, July 1927.

[25]Hartshorn, A. S., "Theoretical Relationship for a Wing with Unbalanced Ailerons," *Reports and Memoranda 1259*, Aeronautical Research Council, London, Oct. 1929.

[26]Pearson, H. A., "Theoretical Span Loading and Moments of Tapered Wings Produced by Aileron Deflection," NACA TN-589, Jan. 1937.

[27]Pearson, H. A., "Span Load Distribution for Tapered Wings with Partial-Span Flaps," NACA TR-585, Nov. 1937.

[28]Pearson, H. A., and Jones, R. T., "Theoretical Stability and Control Characteristics of Wings with Various Amounts of Taper and Twist," NACA TR-635, April 1937.

[29]Filotas, L. T., "Solution of the Lifting Line Equation for Twisted Elliptic Wings," *Journal of Aircraft*, Vol. 8, No. 10, 1971, pp. 835–836.